Transactions, SMiRT-22
San Francisco, California, USA - August 18-23, 2013
Division IX

CREEP RESISTANCE PROPERTIES OF A PHOSPHORUS-DOPED/OXYGEN-FREE COPPER-SILVER ALLOY: EXPERIMENTAL RESULTS AND EMPIRICAL MODEL APPLICATION

Antonietta Lo Conte[1], Federico Bassi[2]

[1] Researcher, Dipartimento di Meccanica, Politecnico di Milano, MILANO

(antonietta.loconte@polimi.it)

[2] Research Fellow, Dipartimento di Meccanica, Politecnico di Milano, MILANO

(federico.bassi1986@gmail.com)

ABSTRACT

The purpose of this work is the study of creep behavior for a phosphorus-doped oxygen-free copper-silver alloy at low temperatures. Experimental tests at different stress and temperature levels will be performed and analyzed in comparison with the equivalent failure tests for a pure ETP copper. The obtained creep curves will be fitted in an empirical model based on the continuum damage mechanics. The aim is to determine material constants and to predict new curves at different stress conditions without the need of additional experimental results. Strain ratio determined during experimental tests has been also proven by a physical model which considers the interested deformation mechanism.

INTRODUCTION

In recent years the choice of materials increased its important role in the design field. This came from innovations in the realization processes of the materials that made available new alloys and composites able to replace or compete with the solutions previously adopted.
The *right* material will accomplish its purpose over a given period, limiting maintenance requirements and be readily available at competitive prices.
In nuclear energy production copper plays an important role because of its electrical and mechanical properties in conductivity and corrosion resistance context. For example nuclear waste canisters are commonly copper designed, since they are placed several meters under ground in a high corrosive location due to water absorption by the surrounding subsoil. Because of radioactive waste, canisters temperature is raised up to 100°C; in this condition copper begins suffer from creep damage.
The use of oxygen free copper alloys could be a solution to these problems since several experimental studies confirm their higher creep resistance properties compared to pure copper.
Empirical and physical models are hereby presented to support the results of experimental creep tests in different copper alloys, in order to understand how state-of-the-art materials can improve the range of applicability of materials in a nuclear energy production context.

CREEP UNIAXIAL TESTS

In this paper a copper ETP (Electrolytic-Tough-Pitch) and a phosphorus doped/oxygen free Cu-Ag alloy (CuAgOF) were analyzed and compared in terms of creep at low temperatures. Creep tests at constant load were conducted and interrupted at 1000 h for CuETP and CuAgOF in order to determine the minimum creep rate in both materials for whom chemical and mechanical

Table 1: Chemical properties of the tested materials

Material	Ni ppm	Zn ppm	Sn ppm	Pb ppm	Fe ppm	Ag ppm	S ppm	P ppm	O_2 ppm
CuETP	15	5	20	5	5	13	0	0	143
CuAg0.1	38	25	60	32	35	1200	12	50	0

Table 2: Mechanical properties of the tested materials at room temperature

Material	$R_{p0.2}$ MPa	R_m MPa	Elongation %
CuETP	327.4	348	12.8
CuAgOF	368.3	383.6	11.0

properties are reported in Tabs 1 and 2. Experiments were conducted on standard specimens with a 25 mm gauge length (Fig. 1) in a 12000 N Satec JE1016 constant load creep test machine. The furnace was controlled in three different areas high, medium and low by three S

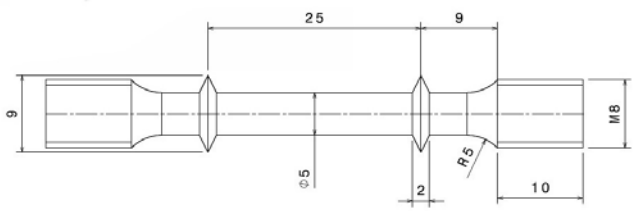

Figure 1: Specimen dimensions

thermocouples with a maximum admitted fluctuation of ± 1°C from the set temperature. The high temperature extensometry of Fig. 2 was used to perform these tests. Strain-time curves

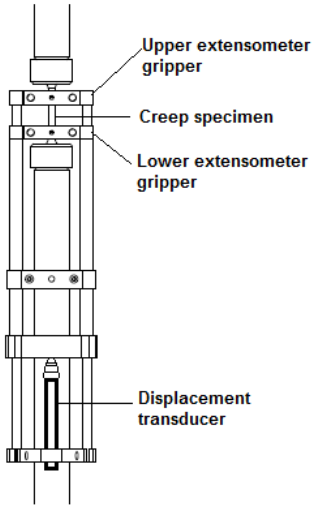

Figure 2: Extensometry equipment

have been determined for both CuETP and CuAgOF under temperature and stress conditions of Tab. 3. As expected the oxygen free copper has better resistance properties given by the significant presence of Phosphorus in the alloy (50 ppm) which reduces the creep ductility. A comparison can be made by observing Fig. 3 where the worst testing condition for CuAgOF causes lower strains than the less critical condition for CuETP.

Table 3: Test conditions and secondarycreep strain rate

Material	**Temp** °C	**Stress** MPa	$\dot{\varepsilon}_{\mathbf{final}}$ 1/h	$\mathbf{t}_f$ h
CuETP	80	133	9.53E-8	
	80	166	1.70E-7	
	100	133	2.98E-7	
	100	166	4.99E-7*	374*
CuAgOF	80	166	8.5E-9	
	100	166	2.35E-7	

* Minimum creep rate, the failure time is less than 1000 h

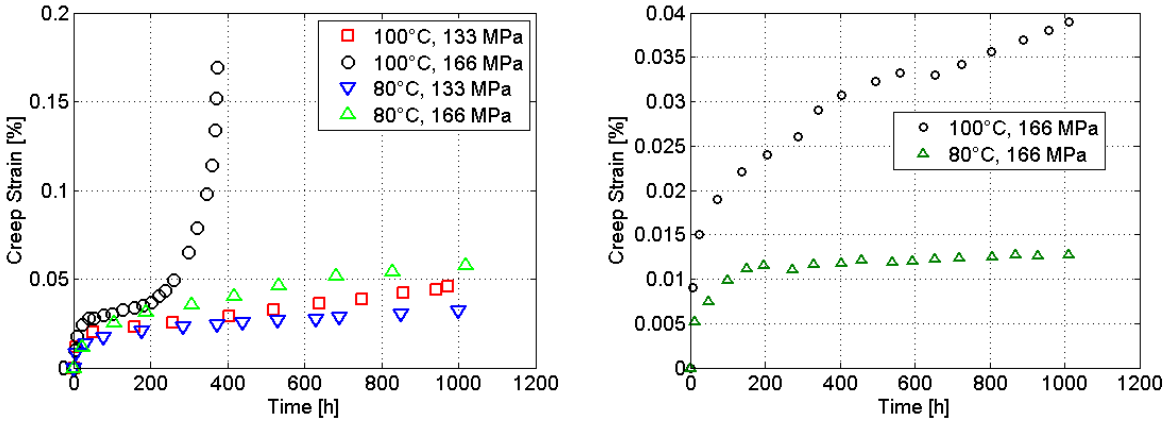

(a) CuETP creep curves

(b) CuAgOF creep curves

Figure 3: Uniaxial time vs. strain curves for Electrolytic-Tough-Pitch and Oxygen-Free/Ag alloyed copper

EMPIRICAL MODEL

When materials are subjected to critical conditions such as cold and work industrial processes, high or low temperatures, and constants loads, microscopic defects could develop and be responsible not only for starting cracks and final ruptures, but also for inducing damage such as reducing strength, toughness, residual life or increasing stress and strain. Mechanical researchers have tried to reproduce the effects of microscopic defects by introducing internal state variables called damage variables, which are based on thermodynamic laws and continuum mechanics. Continuum damage mechanics studies the growth of micro-cavities and their effects on materials' mechanical behavior. Microscopic damage has been macroscopically quantified with the continuum damage mechanics, representing the effects of the distributed defects as internal state variables. Damage tensor ω_{ij} has been created in order to define continuum damage state ($\omega_{ij} = 0$ no damage, $\omega_{ij} = 1$ complete damage). The model used in this paper to predict creep curves is based on creep continuum damage constitutive Eqs. (1) and (2)

$$\dot{\varepsilon}^c_{ij} = \frac{3}{2} A \Big(\frac{\sigma_{eq}}{1-\omega} \Big)^n \frac{S_{ij}}{\sigma_{eq}} t^m \tag{1}$$

$$\dot{\omega} = B \frac{(\alpha\hat{\sigma} + (1-\alpha)\sigma_{eq})^\chi}{(1-\omega)^\phi} t^m \tag{2}$$

where A, n, m, B, χ, ϕ are material constants, σ_{eq} the equivalent stress, ω the damage, S_{ij} the deviatoric stress, α the multiaxial damage parameter, $\hat{\sigma}$ the maximum principal stress and $\dot{\varepsilon}^c_{ij}$ the creep strain rate at a given time t. Eqs. (1) and (2) represent a tri-axial model that can be reduced in its uniaxial form so as to determine the material constants by fitting it to experimental uniaxial creep tests at the same temperature at different stress levels.
After the determination of the material constants it is possible to apply the model in order to evaluate at the same temperature at different stress levels, new uniaxial creep curves. Eqs. (3) and (4) represent the uniaxial creep of materials:

$$\dot{\varepsilon}^c = A\Big(\frac{\sigma}{1-\omega}\Big)^n t^m \tag{3}$$

$$\dot{\omega} = B\frac{\sigma^\chi}{(1-\omega)^\phi} t^m \tag{4}$$

where σ is the applied stress.
These equations can be easily integrated in order to define strain as a function of time and stress:

$$\varepsilon^c = \frac{A\sigma^{(n-\chi)}}{B(\phi+1-n)}\left\{1-\left[1-\frac{B(1+\phi)\sigma^\chi t^{(1+m)}}{1+m}\right]^{1-n/(\phi+1)}\right\} \tag{5}$$

$$= \frac{A\sigma^n t_f^{(1+m)}}{(1+m)[1-n/(\phi+1)]}\left\{1-[1-(t/t_f)^{(1+m)}]^{1-n/(1+\phi)}\right\} \tag{6}$$

where t_f is the time to rupture determined by Eq. (7):

$$t_f = \left[\frac{(1+m)}{B(\phi+1)\sigma^\chi}\right]^{1/(1+m)} \tag{7}$$

It is now possible to substitute $t = t_f$ in Eq. (6) to define the creep failure strain ε^c_f

$$\varepsilon^c_f = \frac{A\sigma^n t_f^{(1+m)}}{(1+m)[1-(n/(\phi+1))]} \tag{8}$$

Eq. (5) represents the creep strain as a function of stress and time. The determination of the material constants, obtained by applying the least squares optimization approach can be quite complicated since there are six dependent variables. A simplified approach (Hyde et al. 1998) comes from the normalization of Eq. (6) with respect to the failure strain of Eq. (8).

$$\frac{\varepsilon^c}{\varepsilon^c_f} = \{1-[1-(t/t_f)^{(1+m)}]^{1-n/(1+\phi)}\} \tag{9}$$

Equation (9) now depends only on three material constants m, n and ϕ which can be obtained by fitting the function to a group of experimental normalized creep curves through the least squares optimization approach. Once the three constants are known, A can be obtained by arranging Eq. (8):

$$A = \varepsilon^c_f \cdot \frac{(1+m)[1-(n/(\phi+1))]}{\sigma^n t_f^{(1+m)}} \tag{10}$$

By re-arranging Eq. (7) it is possible to express stress as a function of the failure time:

$$\log(\sigma) = \log\left\{\left[\frac{B(\phi+1)}{1+m}\right]^{(-1/\chi)}\right\} - \left(\frac{1+m}{\chi}\right)\log(t_f) \tag{11}$$

This function represents a line, so if at least a couple of stress and failure time data are known from two creep experimental curves ($\sigma_1, \sigma_2, t_{f1}$ and t_{f2}), it is possible to find the slope according to Eq. (12) and calculate χ:

$$\frac{\log(\sigma_1) - \log(\sigma_2)}{\log(t_{f1}) - \log(t_{f2})} = -\left(\frac{1+m}{\chi}\right) \tag{12}$$

$$\chi = -(1+m)\frac{\log(t_{f1}) - \log(t_{f2})}{\log(\sigma_1) - \log(\sigma_2)} \tag{13}$$

The intercept i allows to calculate B as shown in Eq. (15):

$$i = -\frac{\log(t_{f2})}{\log(t_{f1}) - log(t_{f2})} \tag{14}$$

$$B = \frac{(1+m)}{(\phi+1)} \cdot e^{-i\chi} \tag{15}$$

This approach is based on the fact that the continuum damage equations well reproduce the strain/time creep curves. This is possible only if the experimental data do not tend to scatter especially in the failure time. In this case, the three variable approach gives a good correlation to the normalized curves.

CuETP

The simplified three variables approach has been applied to bibliography CuETP creep data by RFI 2005 and the experimental results at 100°C described in the ''creep uniaxial tests'' section. Since the model works with strain vs. time curves until rupture, the rupture data at 133 MPa have been obtained by the use of the Larson Miller parameter of the examined material. The couples of strain-time data at 100°C have been fitted to the model in order to determine the continuum damage constitutive equation constants of Tab. 4. Thanks to these constants new creep curves in intermediate stress conditions have been determined in Fig 4.
Fig. 4b shows a less good interpolation with the data because of the initial approximation based on Larson Miller parameter.

Table 4: Creep continuum damage constitutive equation constants for CuETP at 100°C

Dataset	**m**	**n**	ϕ	**A**	χ	**B**
RFI 2005	-0.84	6.07	9.55	9.55E-17	3.06	2.56E-10
tested	-0.64	3.44	3.73	4.35E-11	3.40	2.65E-10

CuOF

Empirical model has been also applied to a set of bibliography data by Sandström et al. (2007) related to creep tests carried on CuOF Copper at 175°C.
In this case the constitutive equation constants are reported in Tab. 5. As observed in Fig. 5 the model allow us to interpolate the experimental creep curves with a significant approximation goodness.

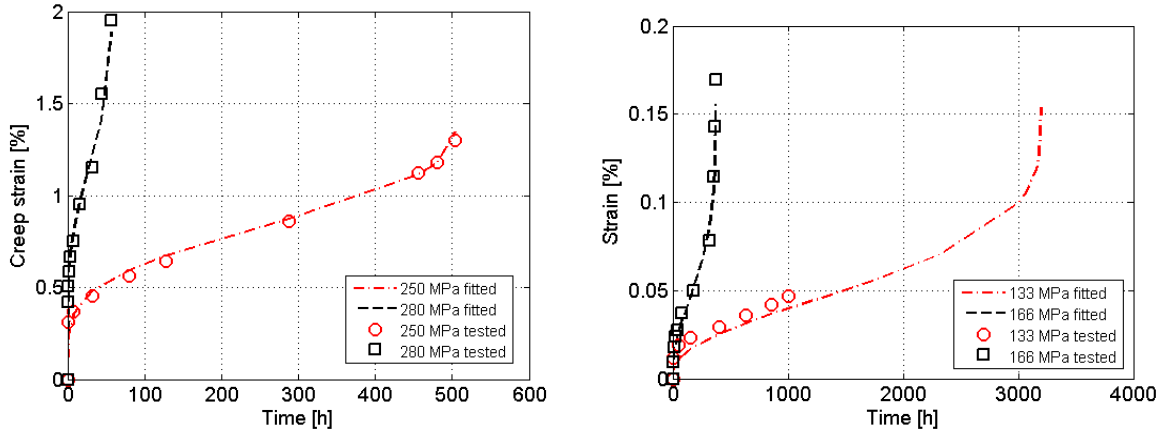

(a) 3 variable approach on CuETP at 100°C. RFI data

(b) 3 variable approach on CuETP at 100°C. Experimental data

Figure 4: 3 variable approach applied to a set of uniaxial creep curves

Table 5: Creep continuum damage constitutive equation constants for CuOF at 175°C

Material	**m**	**n**	ϕ	**A**	χ	**B**
CuOF	-0.72	2.11	4.075	1.61E-7	1.30	1.54E-5

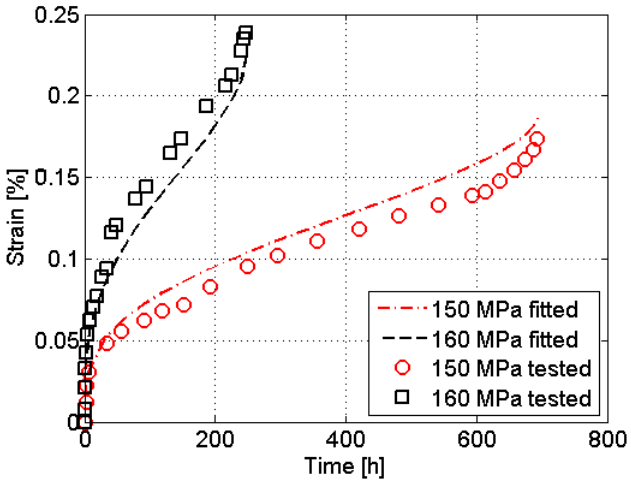

Figure 5: 3 variable approach on Oxygen Free Copper

PHYSICAL MODEL

According to a physical approach for the plastic deformation of a metallic material the total strain rate can be described by the sum of elastic strain rate and creep strain rate as shown in Eq. (16)

$$\frac{d\varepsilon_{TOT}}{dt} = \frac{1}{E}\frac{d\sigma}{dt} + A\sigma_{eff}^{n} \tag{16}$$

where E is the Young's modulus, A and n are constants. σ_{eff} represents the difference between the applied stress σ and the internal back stress σ_i, assumed as a result of work hardening,

$$\sigma_{eff} = \sigma - \sigma_i \tag{17}$$

During plastic deformation ε there is a generation of dislocations which cause the dislocation density ρ to change as follows

$$\frac{d\rho}{dt} = \frac{m}{bL} - 2\omega\rho \tag{18}$$

where m is the Taylor factor, b is the Burgers vector, L the free path of released dislocations and ω a constant. The first term on the right side of the Eq. (18) is the result of work hardening while the second term represents the dynamic recovery. The assumption of dislocation movement governed by forest of dislocations, shows the relation between internal back stress and dislocation density of the type

$$\sigma_i = \alpha G b\sqrt{\rho} \tag{19}$$

where G is the shear modulus. By inserting Eq. (19) into Eq. (18) and grouping the known constants it is possible to express the variation of internal back stress with the strain

$$\frac{d\sigma_i}{d\varepsilon} = \omega(C - \sigma_i) \tag{20}$$

This equation can be directly integrated obtaining

$$\sigma_i = C - C_1 e^{-\omega\varepsilon} \tag{21}$$

C_1 is a constant which can be determined by applying initial conditions of null internal back stress at null strain ($\sigma_i(\varepsilon_i = 0) = 0$) and it is equal to C.

$$\sigma_i = C(1 - e^{-\omega\varepsilon}) \tag{22}$$

This model gives a good description of the plastic deformation for f.c.c.
A common thought is that at temperatures higher than half the melting temperature, deformation is controlled by climb of dislocations. In this case the climb rate can be expressed as a function of the climb mobility M_{climb}

$$v_{climb} = M_{climb} b\sigma \tag{23}$$

According to Hirth and Lothe (1968) the climb mobility depends on the self diffusion coefficient D_{s0}

$$M_{climb} = \frac{D_{s0} b}{k_B T} e^{\frac{\sigma b^3}{k_B T}} \tag{24}$$

where T is the absolute temperature and k_B is the Boltzman constant ($1.3806503 \cdot 10^{-23}[J/K]$). Time dependent recovery of dislocation caused by climb can be related to climb mobility by considering the annihilation of dislocation dipoles and updating Eq. (18)

$$\frac{d\rho}{d\varepsilon} = \frac{m}{bL} - 2\omega\rho - \frac{2}{\dot{\varepsilon}} M_{climb} \tau_L \rho^2 \tag{25}$$

where τ_L is the dislocation line tension. $2\omega\rho$ is ignored since it has more influence at lower temperatures while if a stationary condition is considered a constant dislocation density is assumed $d\rho/d\varepsilon = 0$ with $\sqrt{\rho} = c_L/L$ where c_L is a strain hardening coefficient. Under these conditions it is possible to combine Eqs (25) and (24) in order to define the minimum strain ratio

$$\dot{\varepsilon} = \frac{2bc_L}{m} \frac{D_{s0} b}{k_B T} e^{\frac{\sigma b^3}{k_B T}} \tau_L \rho^{3/2} \tag{26}$$

By inserting Eq. (19) into (26) it is possible to notice that $\dot{\varepsilon}$ changes as σ^3 i.e. the Norton exponent takes a value of 3. In fact the exponential term gives only a small effect.
However at lower temperatures deformation is controlled by glide of dislocations and model of Eq. (26) can no longer describe correctly the strain ratio. In this case a relationship between the glide of dislocations through an obstacle field has been found by Kocks et al. (1975)

$$\frac{d\varepsilon}{dt} = f\sigma^2 e^{-\frac{Q_{eff}}{RT}\left[1-\left(\frac{\sigma}{\sigma_{BS}}\right)^{q_1}\right]^{q_2}} \tag{27}$$

where q_1 and q_2 are constants related to the shape and distribution of the obstacles to flow experimentally assumed. σ_{BS} is the maximum back stress, R is the universal gas constant and Q_{eff} is the activation energy for self diffusion. Eqs (27) and (26) can be finally combined in order to determine a physical model for copper valid at both low and high temperatures.

$$\dot{\varepsilon} = \frac{2bc_L}{m}\frac{D_{s0}b\tau_L}{k_BT}\left(\frac{\sigma}{\alpha mGb}\right)^3 e^{\frac{\sigma b^3}{k_BT}} e^{-\frac{Q_{\text{eff}}}{RT}\left[1-\left(\frac{\sigma}{\sigma_{BS}}\right)^{q_1}\right]^{q_2}} \tag{28}$$

This model gives the minimum creep strain ratio during steady-state creep for pure copper considering the fundamental process of climb and glide, without the use of fitting parameters.
In Oxygen Free copper the model is equally valid after the introduction of the experimental coefficient f_P which takes into account the presence of Phosphorus in the alloy

$$\dot{\varepsilon} = \frac{2bc_L}{m}\frac{D_{s0}b\tau_L}{k_BT}\left(\frac{\sigma}{\alpha mGb}\right)^3 e^{\frac{\sigma b^3}{k_BT}} e^{-\frac{Q_{\text{eff}}}{RT}\left[1-\left(\frac{\sigma}{\sigma_{BS}}\right)^{q_1}\right]^{q_2}} / f_P \tag{29}$$

In order to apply the physical model with the aim to describe the minimum creep rate for CuETP and CuAgOF at the same temperature and stress conditions of the experimental tests of Fig. 3, the maximum back stress has been calculated according to Nembach (1996) in relation to its physical meaning:

$$\sigma_{BS} = \frac{1}{bR_l}\cdot\frac{Gb^2}{4\pi(1-\nu)}\cdot\left[(1+\nu)\cos^2\theta + (1-2\nu)\sin^2\theta\right]\cdot\log\left(\frac{4R_l}{e\cdot b}\right) \tag{30}$$

where R_l is the radius of curvature of a dislocation between two pinning centers, ν is the Poisson constant and θ is the angle between the Burgers vector and the vector of unit length parallel to the local direction of the dislocation line. The radius of curvature can be calculated as

$$R_l = \frac{L}{1.47} \tag{31}$$

L can depend on the grain size, the subgrain size or the interaction distance between dislocations

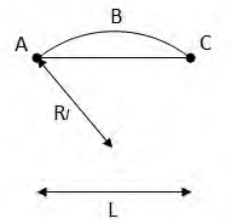

Figure 6: Dislocation mobility

L. In the last case it can be expressed as a function of the dislocation density $\rho[1/m^2]$ according to Hallgren et al. (2012):

$$L = \frac{c_L}{\rho^{\phi}} \tag{32}$$

where usually $\phi = 0.5$ and c_L is typically much larger than unit. In the other situations, if the spurt distance L is related to the grain size d_{grain}, $c_L = d_{grain}$ and $\phi = 0$. Otherwise if the subgrain size d_{sub} determines L and there is a fixed distance h between the dislocation in the sub-boundaries, $L = 1/h\rho_{sub}$ where ρ_{sub} is the dislocation density in the sub-boundaries, and $c_L = 1/h$ and $\phi = 1$.
The dislocation density has been expressed in relation to the shear yield stress τ

$$\tau = \alpha G b \sqrt{\rho} \tag{33}$$

where α is the same constant of Eq. (28) and can be evaluated by taking into account the average of a set of edge dislocations $1/2\pi(1-\nu)$ and a set of screw dislocations $1/2\pi$

$$\alpha = \frac{(1-\nu/2)}{2\pi(1-\nu)} = 0.19 \tag{34}$$

The shear yield stress was calculated by using Eq. (35).

$$\tau = \sigma_y m \tag{35}$$

With Eq. (33) it is now possible to evaluate dislocation densities for copper ETP and oxygen free.
The parameter values listed in Tab. 6 took to the results of Fig. 7, where minimum creep strain ratio of the experimental tests and RFI dataset are compared to the corresponding data obtained with the physical model.

Table 6: Parameter values for CuETP and CuAgOF used in the physical model

Parameter	**Material**	**Value CuETP**	**Reference**
D_{s0}	CuETP	2E-5 m^2/s	Ashby et al. (1982)
	CuAgOF	2.7E-5 m^2/s	Read et al. (1974)
Q_eff	CuETP	197000 J/mol	Ashby et al. (1982)
	CuAgOF	185000 J/mol	Read et al. (1974)
b		2.56E-10 m	
m		3.06	
ν		0.34	
α		$(1-\nu/2)/(2\pi(1-\nu))$=0.2	
σ_{BS}	CuETP	425 MPa	Nembach (1996)
	CuAgOF	466 MPa	"
τ_L		$Gb^2/2$=1.43E-9 MPa	Dieter (1986)
ρ	CuETP	2.29E15 $1/m^2$	
	CuAgOF	2.90E15 $1/m^2$	
G		$G_0(1-0.54(T-300)/T_{melting})$; G_0=43657 MPa	Ashby et al. (1982)
f_P	CuAgOF	3000	
c_L		54	
q_1		1.89E-2	
q_2		6.84E-2	

CONCLUSIONS

Creep tests of copper ETP and copper-silver oxygen free alloy have been performed. CuAgOF has shown better creep resistance properties because of the presence of phosphorus in its alloy which reduces the creep ductility. For both materials experimental tests have been fitted to an empirical model based on continuum damage mechanics to determine six material constants which are able to reproduce complete creep curves in the stress range defined during the fitting procedure.

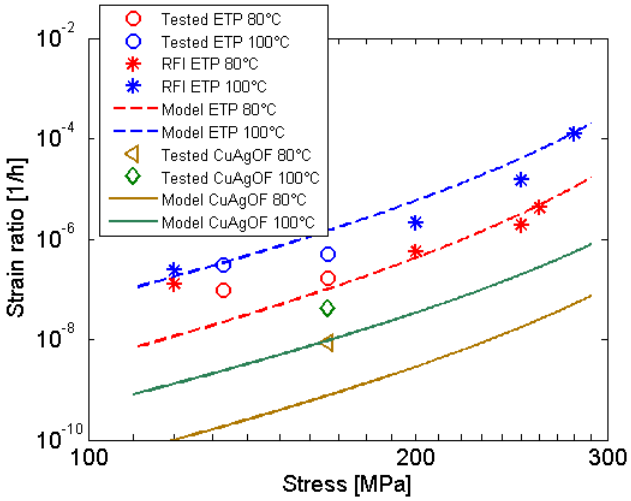

Figure 7: Minimum creep strain ratio for CuETP and CuAgOF at different stress conditions

A physical model has been discussed in order to determine the secondary creep strain ratio without the use of fitting parameters. The results of the model application have been compared to the experimental data and showed not only a lower strain ratio of CuAgOF than CuETP at the same temperature and stress conditions, but also its lower variation in the strain ratio in function of the applied stress variation.
The approximation goodness is better with CuETP because of its high purity which decreases the errors given by the scatter of the physical constants related to the micro-structural composition which slightly effects the results for the CuAgOF alloy.

REFERENCES

Ashby, M.F., Kocks, U.F. and Argon, A.S. (1975). *Prog. Mater. Sci.* 19, 1.

Ashby, M. F. and Frost, H. J. (1982). *Deformation mechanism maps. The plasticity and creep of metals and ceramics*, Pergamon Press.

Dieter, G.E. (1986). *Mechanical Metallurgy*, McGraw-Hill.

Hallgren, J. and Sandströ, R. (2012). ''The role of creep in stress strain curves for copper'', *J. Nuclear Materials*, 422(12), 51-57.

Lothe, J. and Hirth, J.P. (1968). *Theory of Dislocations*, McGraw-Hill.

Nembach, E. (1996). *Particle Strengthening of Metals and Alloys*, Wiley-Interscience.

Read, M.E., Butrymowicz, D.B.and Manning, J.R. (1974). ''Diffusion in Copper and Copper Alloys Part II. Copper-Silver and Copper-Gold Systems'', *J. Phys. Chem Ref. Data*, Vol 3, 527-595.

RFI (in Italian) - Rete Ferroviaria Italiana (2005). ''Nuovi conduttori per linee di contatto''.

Sun, W. , Hyde, T.H. and Tang, A. (1998). ''Determination of material constants in creep continuum damage constitutive equations'', *Strain*, (August 1998), 83-90.